AMERICAN SOCIETY FOR MICROBIOLOGY | Journal of Virology®

VIRUS-CELL INTERACTIONS

IFI16 Partners with KAP1 to Maintain Epstein-Barr Virus Latency

Huanzhou Xu,[a] Xiaofan Li,[a]* Beth A. Rousseau,[a] Ibukun A. Akinyemi,[b] Tiffany R. Frey,[b] Kevin Zhou,[a] Lauren E. Droske,[a] Jennifer A. Mitchell,[b] Michael T. McIntosh,[b,c] Sumita Bhaduri-McIntosh[a,c]

[a]Division of Infectious Diseases, Department of Pediatrics, University of Florida, Gainesville, Florida, USA
[b]Child Health Research Institute, Department of Pediatrics, University of Florida, Gainesville, Florida, USA
[c]Department of Molecular Genetics and Microbiology, University of Florida, Gainesville, Florida, USA

ABSTRACT Herpesviruses establish latency to ensure permanent residence in their hosts. Upon entry into a cell, these viruses are rapidly silenced by the host, thereby limiting the destructive viral lytic phase while allowing the virus to hide from the immune system. Notably, although the establishment of latency by the oncogenic herpesvirus Epstein-Barr virus (EBV) requires the expression of viral latency genes, latency can be maintained with a negligible expression of viral genes. Indeed, in several herpesviruses, the host DNA sensor IFI16 facilitated latency via H3K9me3 heterochromatinization. This silencing mark is typically imposed by the constitutive heterochromatin machinery (HCM). The HCM, in an antiviral role, also silences the lytic phase of EBV and other herpes viruses. We investigated if IFI16 restricted EBV lytic activation by partnering with the HCM and found that IFI16 interacted with core components of the HCM, including the KRAB-associated protein 1 (KAP1) and the site-specific DNA binding KRAB-ZFP SZF1. This partnership silenced the EBV lytic switch protein ZEBRA, encoded by the *BZLF1* gene, thereby favoring viral latency. Indeed, IFI16 contributed to H3K9 trimethylation at lytic genes of all kinetic classes. In defining topology, we found that IFI16 coenriched with KAP1 at the *BZLF1* promoter, and while IFI16 and SZF1 were each adjacent to KAP1 in latent cells, IFI16 and SZF1 were not. Importantly, we also found that disruption of latency involved rapid downregulation of IFI16 transcription. These findings revealed a previously unknown partnership between IFI16 and the core HCM that supports EBV latency via antiviral heterochromatic silencing.

IMPORTANCE The interferon-gamma inducible protein 16 (IFI16) is a nuclear DNA sensor that mediates antiviral responses by activating the inflammasome, triggering an interferon response, and silencing lytic genes of herpesviruses. The last, which helps maintain latency of the oncoherpesvirus Epstein-Barr virus (EBV), is accomplished via H3K9me3 heterochromatinization through unknown mechanisms. Here, we report that IFI16 physically partners with the core constitutive heterochromatin machinery to silence the key EBV lytic switch protein, thereby ensuring continued viral latency in B lymphocytes. We also find that disruption of latency involves rapid transcriptional downregulation of IFI16. These findings point to hitherto unknown physical and functional partnerships between a well-known antiviral mechanism and the core components of the constitutive heterochromatin machinery.

KEYWORDS herpesvirus, Epstein-Barr virus, latency, IFI16, KAP1, TRIM28, heterochromatin machinery, H3K9me3, ZEBRA, ZTA

Interferon-gamma inducible protein 16 (IFI16) is a nuclear sensor of viral genomes, including those of the human papillomavirus and herpesviruses (1–3). Upon detecting viral DNA, IFI16 activates the inflammasome and facilitates the stimulator of interferon genes (STING) and interferon regulatory factor (IRF3)-mediated interferon (IFN)-β response (4, 5). Aside from triggering these innate immune responses, IFI16 also silences incoming genomes of herpesviruses, including herpes simplex virus (HSV), human cytomegalovirus (CMV), and Kaposi's sarcoma-associated herpesvirus (KSHV) (6–11). For the host, silencing of the productive phase

Editor Felicia Goodrum, University of Arizona

Address correspondence to Sumita Bhaduri-McIntosh, sbhadurimcintosh@ufl.edu.
*Present address: Xiaofan Li, HIV and AIDS Malignancy Branch, National Cancer Institute, National Institutes of Health, Bethesda, Maryland, USA.
The authors declare no conflict of interest.
Received 29 June 2022
Accepted 25 July 2022
Published 15 August 2022

of the virus limits pathology; while for the virus, gene silencing may allow the virus to remain dormant, which for herpesviruses enables them to establish latency. In the case of the herpesvirus Epstein-Barr virus (EBV), the Chandran lab showed that EBV lytic genes of all kinetic classes were silenced by IFI16, and depletion of IFI16 during reactivation from latency resulted in amplification of the EBV lytic phase (12). Thus, in addition to inflammatory and IFN responses, IFI16 functions in an important antiviral capacity by silencing foreign DNA genomes.

While IFI16's antiviral function is important to both virus and host, the mechanisms by which IFI16 transcriptionally silences foreign/viral DNA are not well understood. That said, studies by several labs point to some key features. One of these is the ability of IFI16 to distinguish between self and foreign genomes (4, 5, 7, 9, 13). Second, IFI16 nucleates on viral DNA (3), which is sometimes observable as filamentous structures (14), through homotypic interactions of its pyrin domain (15). Third, while IFI16 silences herpesviral (HSV-1) genes by excluding RNA polymerase II and transcription factors TATA-binding protein and Oct1, it can simultaneously activate host genes (3). Fourth, IFI16 silences herpesviral lytic genes by facilitating their heterochromatinization through trimethylation of histone 3 at lysine 9 (3, 10). These last two observations suggest that IFI16 functions with other proteins to silence genes and is supported by the fifth observation that IFI16 recruits the histone methyl transferases SUV39H1 and GLP to silence lytic genes of KSHV (16). Thus, IFI16 may function as part of a larger multiprotein machinery to sense and silence herpesviral genomes in the nucleus, potentially helping to establish viral latency.

Once established, herpesviral latency must be maintained to ensure lifelong viral persistence. In addressing its contribution to the maintenance of herpesvirus latency, IFI16 was found to silence EBV lytic genes in latently infected B lymphoma cell lines (12). EBV infects $>$95% of humans and is causally linked to several cancers, including endemic Burkitt lymphoma (BL) in African children, B lymphoproliferative diseases (LPD)/lymphomas in immunocompromised hosts, and nasopharyngeal cell carcinoma in the Far East, as well as to the autoinflammatory and neurodegenerative disease multiple sclerosis (17–22). Although EBV infects both B and epithelial cells, it persists in a latent state in B lymphocytes. Notably, EBV cancers harbor the virus in its latent state. In healthy individuals, latent EBV reactivates periodically into the lytic phase to produce an infectious virus, seeding new B cells and new hosts. Indeed, the productive/lytic and dormant/latent phases are both important for EBV-related diseases and persistence in the population.

The availability of convenient latent and lytic EBV cell culture models has greatly facilitated studies of the establishment and maintenance of herpesviral latency, as well as lytic reactivation. In contrast to the establishment of EBV latency, which requires both viral (latent membrane proteins and Epstein-Barr nuclear antigens) and cellular factors, latency can be maintained with minimal to no viral protein expression as evidenced by latency I (EBNA 1 only expression, observed in BL) and latency 0 (no viral protein expression, observed in healthy hosts). The host, however, plays an important role in silencing lytic genes to maintain the latent state. In that context, the constitutive heterochromatin machinery (HCM) that tightly regulates endogenous retroviral elements and pericentromeric repeats also silences EBV and KSHV lytic genes to establish and maintain latency (23–27). This machinery imposes the constitutive heterochromatin mark H3K9me3 with the help of the corepressor KRAB-associated protein 1 (KAP1/TRIM28/TIF1β). A core component of this machinery, KAP1 recruits repressive histone modifiers to silence target DNA. However, lacking a DNA binding domain, KAP1 is directed to DNA usually by members of the Krüppel-associated box (KRAB) domain–zinc finger protein (ZFP) family. In this way, the HCM silences lytic genes of several herpesviruses, thereby serving as a barrier to the lytic phase and enforcing viral latency. With IFI16 found to silence EBV lytic genes (12), IFI16-mediated herpesviral gene silencing linked to H3K9me3 marks, and the HCM known to silence gene expression via H3K9me3, we investigated if IFI16 partnered with the core components of the HCM to silence the EBV lytic phase.

We report here that IFI16 interacts with KAP1 to silence EBV lytic genes. In latently infected cells, IFI16 complexes with KAP1, the KRAB-ZFP SZF1, and K9 trimethylated H3, and these coenrich on the promoter of *BZLF1* that encodes the viral lytic switch. We also defined the spatial relationship between IFI16 and HCM components KAP1 and SZF1 in latently

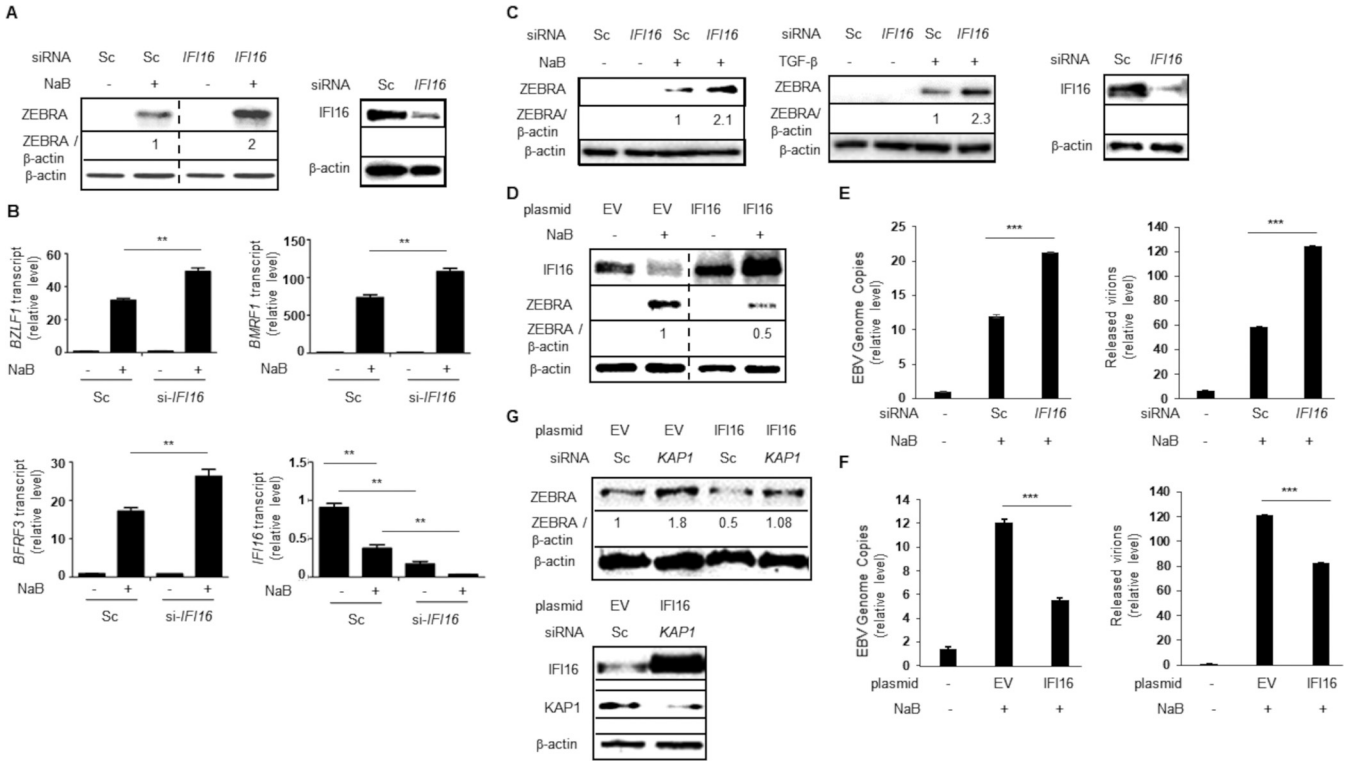

FIG 1 IFI16 partners with KAP1 to silence the EBV lytic state. (A and B) HH514-16 BL cells were transfected with control scrambled siRNA (Sc) or siRNA targeting *IFI16*, exposed to NaB (sodium butyrate; lytic trigger) after 18 h, harvested after another 24 h, and immunoblotted with indicated antibodies (A) or subjected to RT-qPCR analysis of EBV lytic genes of all kinetic classes (*BZLF1*, immediate early; *BMRF1*, early; and *BFRF3*, late) using the $\Delta\Delta C_T$ method after normalization to 18S rRNA (B). Error bars, SEM of three technical replicates and two biological replicates; **, $P < 0.01$. (C) Mutu I BL cells were transfected with control scrambled siRNA (Sc) or siRNA targeting IFI16, exposed to NaB (left) or TGF-β1 (middle) after 18 h, harvested after another 24 h, and immunoblotted with indicated antibodies. (D) HH514-16 BL cells were transfected with empty vector (EV) or IFI16 plasmid, exposed to NaB after 18 h, and harvested after another 24 h before performing immunoblotting with indicated antibodies. (E and F) HH514-16 BL cells were transfected with siRNA targeting *IFI16* (versus scrambled RNA as control) (E) or IFI16 plasmid (versus empty vector [EV] as control) (F), exposed to NaB after 20 h, and harvested after another 36 h (F, left) or 48 h (E and F, right) for qPCR analysis of cell-associated viral genomes (left) or released viral genomes following DNase treatment (right). (G) HH514-16 BL cells were transfected with empty vector (EV), IFI16 plasmid, control scrambled siRNA, or siRNA targeting *KAP1*, exposed to NaB after 18 h, and harvested after another 24 h before immunoblotting with indicated antibodies. Numbers indicate the relative amounts of ZEBRA protein after normalization to β-actin levels. These experiments were performed at least twice.

infected cells and those refractory to lytic triggers. Importantly, we find that disruption of latency is also associated with rapid transcriptional downregulation of IFI16.

RESULTS

IFI16 supported EBV latency. A prior study demonstrated that IFI16 contributed to the maintenance of EBV latency in Burkitt lymphoma cell lines (12). The mechanism of this lytic silencing remains unclear as does whether interference with IFI16 is sufficient to disrupt latency. We, therefore, focused on experimental manipulation of Burkitt lymphoma cells that were tightly latent at baseline but in which the virus could be readily triggered to enter the lytic phase. Consistent with the earlier report, we found that depletion of IFI16 in two distinct BL cell lines, HH514-16 and Mutu I, resulted in enhanced expression of the viral lytic switch protein ZEBRA (BamHI Z EBV replication activator) in response to lytic triggers NaB and tumor growth factor (TGF)-β (Fig. 1A and C). This boost in ZEBRA expression in IFI16-depleted cells compared to cells with unperturbed IFI16 correlated with statistically significant increases in transcripts from EBV lytic genes of all kinetic classes (*BZLF1*, immediate early gene encoding ZEBRA; *BMRF1*, early gene encoding EA-D; *BFRF3*, late gene encoding small viral capsid antigen) (Fig. 1B). In contrast to Fig. 1A and C, overexpression of IFI16 resulted in blunting of the ZEBRA response to the lytic trigger (Fig. 1D). Thus, like the earlier study, we found that IFI16 functioned in a prolatent manner.

Several additional observations resulted from these experiments. First, while IFI16 supported latency, interference with IFI16 was not sufficient to disrupt latency (Fig. 1A to C).

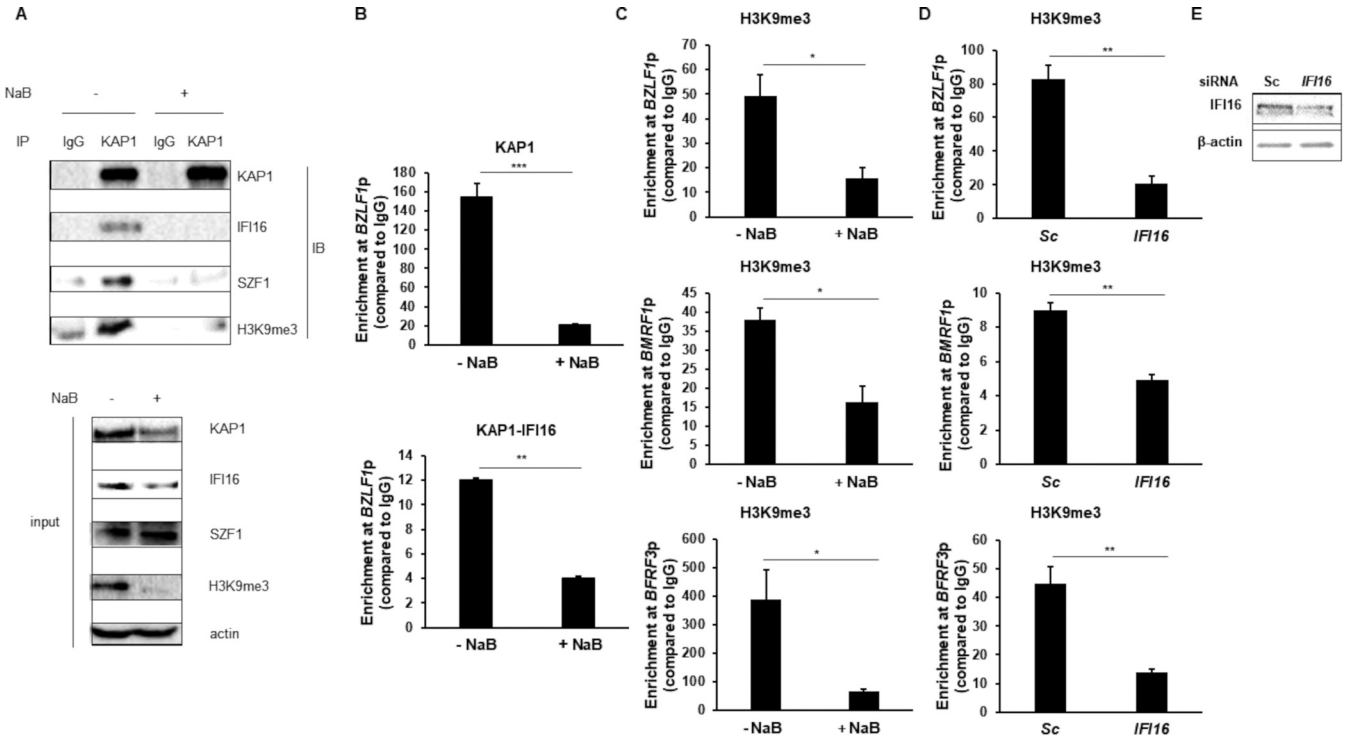

FIG 2 KAP1 and IFI16 coenriched with H3K9me3 and at the *BZLF1* promoter, preferentially in latent cells. (A) HH514-16 BL cells were left untreated or exposed to NaB. After 24 h, lysates were immunoprecipitated (IP) with anti-KAP1 antibody versus control IgG and immunoblotted with indicated antibodies. Input represents 5% of the sample. (B) HH514-16 BL cells were treated with or without NaB for 24 h followed by ChIP-re-ChIP. Chromatin was precipitated using rabbit anti-KAP1 or a control rabbit IgG antibody (top) and subjected to the second round of ChIP using mouse anti-IFI16 or a control mouse IgG antibody (bottom). Extracted DNA was analyzed by qPCR using primers spanning the known KAP1 enrichment site on the *BZLF1* promoter and normalized to input. (C) HH514-16 BL cells were treated with or without NaB for 6 h followed by ChIP using an anti-H3K9me3 antibody or control IgG. (D) HH514-16 BL cells were transfected with control scrambled siRNA (Sc) or siRNA targeting *IFI16* for 18 h (and harvested for immunoblotting in E) or exposed to NaB, harvested after 12 and 24 h, and chromatin was immunoprecipitated with an anti-H3K9me3 antibody or control IgG. Primer sets targeting *BZLF1*, *BMRF1*, and *BFRF3* promoters were used for qPCR in C and D. Error bars, SEM of the means of three independent experiments; *, $P < 0.05$; **, $P < 0.01$; ***, $P < 0.001$.

Second, despite robust lytic activation in response to a strong lytic trigger, an even further synergistic enhancement of lytic gene expression was possible by interfering with IFI16 (Fig. 1B), supporting the idea that IFI16 contributed to the previously described refractory phenotype of latently infected B cells (28–30). Third, we observed a significant reduction in IFI16 message and protein levels following lytic trigger exposure (Fig. 1B and D). While the study by Pisano et al. (12) reported a loss of IFI16 protein after 48 to 72 h of exposure to lytic triggers, we observed this loss earlier (by 24 h) in both transcript and protein levels. Fourth, even when highly overexpressed, IFI16 was unable to abrogate the expression of ZEBRA (Fig. 1D), suggesting that IFI16 functioned with other proteins to silence *BZLF1*. Lastly, depletion of IFI16 also enhanced viral genome replication and release of virions while overexpression of IFI16 had the opposite effect (Fig. 1E and F).

IFI16 partnered with the constitutive heterochromatin machinery, favoring latency. Knowing that IFI16 silenced herpesviral lytic genes via H3K9me3 marks and that the HCM is known to silence EBV lytic genes via H3K9me3 heterochromatinization, we investigated the relationship between IFI16 and the core HCM component KAP1. We found that, while overexpression of IFI16 blunted ZEBRA expression, ZEBRA level recovered to baseline if KAP1 was simultaneously depleted, indicating that IFI16-mediated silencing of ZEBRA required KAP1 (Fig. 1G). With IFI16 now functionally linked to the core HCM, we asked if IFI16 physically interacted with the HCM. Figure 2A shows that, in latently infected cells, IFI16 was complexed with KAP1 and with the KRAB-ZFP SZF1 and histone H3 trimethylated at lysine 9. Notably, upon activation of the lytic cycle, this four-way interaction was largely disrupted and was accompanied by expected reductions in the total levels of KAP1, IFI16, and H3K9me3 (Fig. 2A, input). We believe that the efficient pulldown of KAP1, despite a drop in KAP1 levels after NaB treatment (input), was because KAP1's relationship to other proteins,

including those in the HCM, was likely making it more accessible to the antibody. It is indeed fortuitous that KAP1 precipitated well after NaB treatment. If less KAP1 were to be precipitated following NaB treatment, the coimmunoprecipitation would be uninterpretable.

While H3K9me3 pulldown in the co-immunoprecipitation experiment in Fig. 2A suggested that IFI16 interacted with the HCM on DNA, we sought direct evidence for interaction on the *BZLF1* promoter by performing ChIP-re-ChIP/sequential ChIP. Here, we sequentially precipitated DNA by antibodies to KAP1 and IFI16 and amplified the *BZLF1* promoter, which we know is silenced by the HCM (24, 27). As shown in Fig. 2B, KAP1 and IFI16 coenriched at the *BZLF1* promoter, but this coenrichment was significantly diminished upon lytic activation. To confirm that heterochromatin relaxed upon lytic induction, we performed ChIP with an anti-H3K9me3 antibody on lytically induced and uninduced BL cells. We found that, compared to uninduced cells, H3K9me3 enrichment at representative promoters of all three kinetic classes of EBV genes was diminished in NaB-exposed cells (Fig. 2C). *BMRF1* is an early gene and *BFRF3* is a late gene. To assess the contribution of IFI16 to the enrichment of H3K9me3 marks at lytic promoters, we performed ChIP with an anti-H3K9me3 antibody on induced BL cells transfected with siRNA targeting *IFI16* or scrambled siRNA. We found that the knockdown of IFI16 reduced the enrichment of H3K9 trimethylated marks at lytic promoters compared to control siRNA exposed cells (Fig. 2D). As expected, siRNA targeting *IFI16* resulted in depletion of IFI16 (Fig. 2E). Collectively, these experiments indicated that IFI16 functions with the HCM to block expression of lytic genes of all kinetic classes, including *BZLF1*, which encodes the lytic switch protein, thereby promoting latency.

IFI16 was adjacent to the corepressor KAP1 preferentially in latent/refractory cells. The HCM is recruited by the DNA binding KRAB-ZFP SZF1 to the latent EBV genome via specific binding sites on the genome (24). The association of IFI16, another DNA-binding protein, with the HCM complex raised questions about the structural arrangement of IFI16 and SZF1 in relation to the core component KAP1, which is known to directly interact with SZF1 (27). To address if IFI16 was also adjacent to KAP1, we performed a proximity ligation assay (PLA) followed by immunofluorescence by using EBV seropositive human reference serum to distinguish latent and lytic cells. PLA is an *in situ* assay to detect closely associated proteins observable as a fluorescent focus whenever two proteins of interest are within 40 nm of each other (31). In Fig. 3A, the high number of PLA foci in each nucleus indicated that IFI16 and KAP1 were nearby/adjacent to each other in latently infected cells. In contrast, while latent/refractory cells continued to demonstrate IFI16-KAP1 interactions, such interactions were lost in lytic ZEBRA$^+$ cells (Fig. 3B). As expected, lack of one or both anti-IFI16 and anti-KAP1 antibodies failed to result in PLA foci (Fig. 3C). Notably, however, while KAP1 and SZF1 were known to be adjacent in latent/refractory cells and KAP1 and IFI16 showed adjacency in latent/refractory cells (Fig. 3A), IFI16 and SZF1, although part of the same complex, were not nearby (Fig. 3D).

Lytic activation resulted in rapid depletion of steady-state levels of the *IFI16* message. IFI16's participation with the HCM to silence lytic genes during latency suggested that this mechanism was disrupted to enhance the lytic phase. Indeed, both protein and message levels of IFI16 declined significantly within the first 24 h of exposure to a lytic trigger (Fig. 1B and C). This prompted time course experiments within 24 h of exposure to lytic triggers. As shown in Fig. 4A, IFI16 protein levels declined rapidly by 4 h, reaching a nadir between 8 and 12 h of exposure to a lytic trigger in EBV$^+$ BL cells. Expression of ZEBRA followed soon thereafter, indicating that a lytic activation-related, but ZEBRA-unrelated, mechanism likely caused depletion of IFI16 levels. However, reduction in IFI16 following expression of doxycycline-inducible ectopic ZEBRA also indicated a ZEBRA-dependent mechanism of IFI16 depletion (Fig. 4B).

To assess whether the ZEBRA-independent mechanism resulted from lytic cycle activation or exposure to a histone deacetylase (HDAC) inhibitor, we tested the same HDAC inhibitor NaB on an EBV negative B lymphoma cell line, BJAB. A lack of IFI16 depletion after exposure of EBV$^-$ cells to NaB (Fig. 4C) supported the idea that IFI16 loss was related to lytic cycle activation of viral genomes and was less likely to be related to the presence of an HDAC inhibitor.

Given the rapid, early loss of IFI16 protein after exposure of EBV$^+$ BL cells to a lytic trigger, we also examined steady-state levels of *IFI16* transcripts and found an early decline that corresponded to the decline in IFI16 protein levels (Fig. 4D). We observed a similar

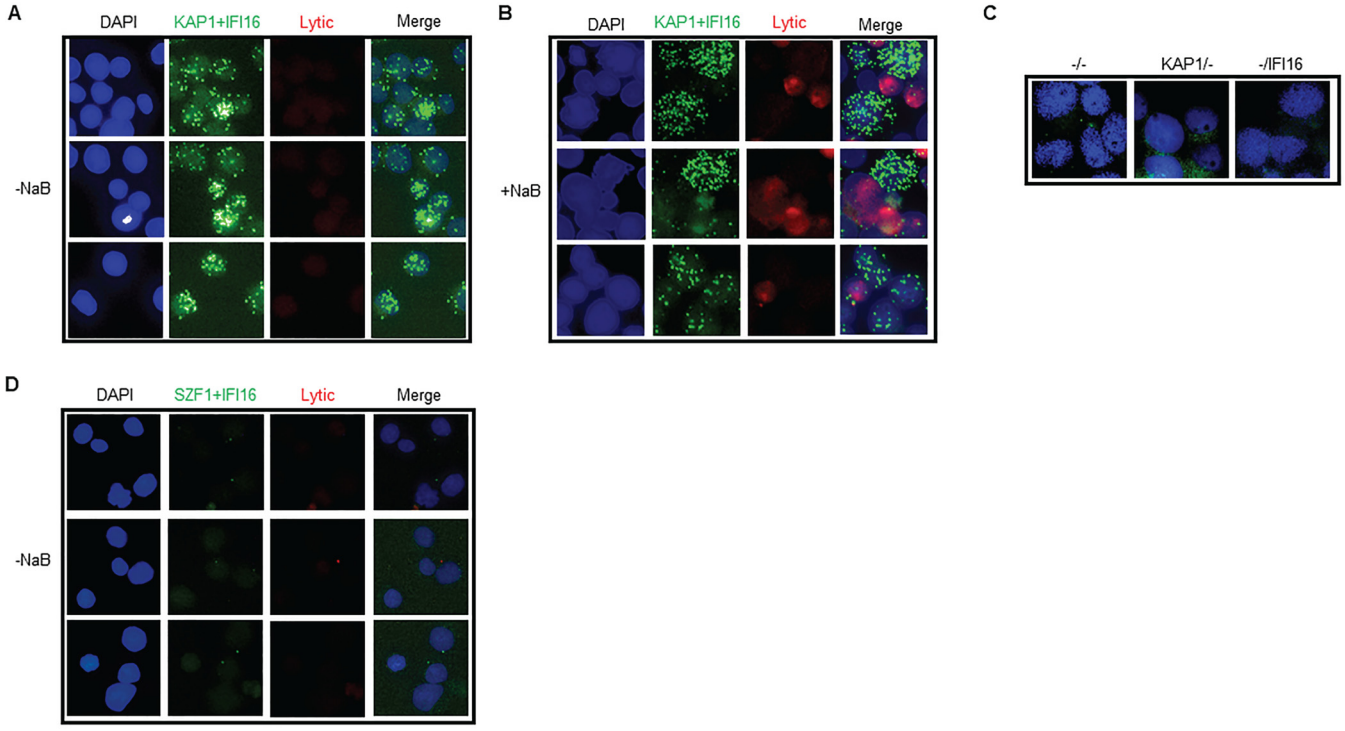

FIG 3 IFI16 was adjacent to KAP1 but not SZF1 in latent cells. HH514-16 BL cells were not induced or induced with NaB for 24 h before performing a proximity ligation assay (PLA) using antibodies targeting KAP1, IFI16, and SZF1. EBV seropositive human reference serum followed by APC-conjugated goat anti-human IgG was used to stain lytic cells (A, B, and D). Negative-control staining in the absence of anti-KAP1, anti-IFI16, or both antibodies is shown in (C). Green foci, *in situ* interactions between KAP1 and IFI16. The experiment was performed at least 3 times. Three representative fields from two independent experiments are shown in A, B, and D.

early decline in *IFI16* transcripts after exposure to trichostatin A (TSA), another HDAC inhibitor known to activate the EBV lytic phase (Fig. 4E). Significantly, however, IFI16 transcript levels remained unchanged after exposure to a third HDAC inhibitor valproic acid (VPA), which is known not to activate the EBV lytic phase (Fig. 4F) (32, 33). Taken together, these experiments point toward a lytic activation-related mechanism of IFI16 depletion that was unrelated to HDAC inhibition *per se*.

Reduced synthesis resulted in an early drop in the abundance of *IFI16* transcripts. In investigating the mechanism of the decline of the *IFI16* transcript, we examined a nascent transcriptomic study in EBV$^+$ BL cells, which we had previously published (34). We found that within 24 h of exposure of cells to the same lytic trigger as in the present study, there was a decline in *IFI16* transcription. We, therefore, investigated if the decline in steady-state levels of *IFI16* transcripts observed in Fig. 4 indeed resulted from reduced RNA synthesis. To test synthesis, we immune-enriched nascent transcripts following incorporation of 5-Bromouridine (BrU) and then amplified *IFI16* nascent transcripts using two different sets of primers and RT-qPCR. We found that, compared to latently infected cells, exposure to the lytic trigger for 10 h resulted in ~60% to 70% reduction in nascent *IFI16* transcripts (Fig. 5A). This suppression was consistent with the ~80% reduction in steady-state *IFI16* message observed at 12 h post-exposure to lytic trigger in Fig. 4D. As expected, lytic activation resulted in expression of *BZLF1* transcripts (Fig. 5B).

Thus, IFI16 participated with the constitutive heterochromatin machinery to maintain EBV latency, and lytic activation was associated with a rapid decline in IFI16 transcription that contributed to the disruption of latency. A model depicting the spatial and functional relationship of IFI16 with core components of the HCM and the EBV genome in latently infected cells is shown in Fig. 6.

DISCUSSION

While IFI16-mediated silencing is associated with H3 trimethylation at lysine 9, how IFI16 recruits the machinery that imposes such silencing marks is mostly unclear. In

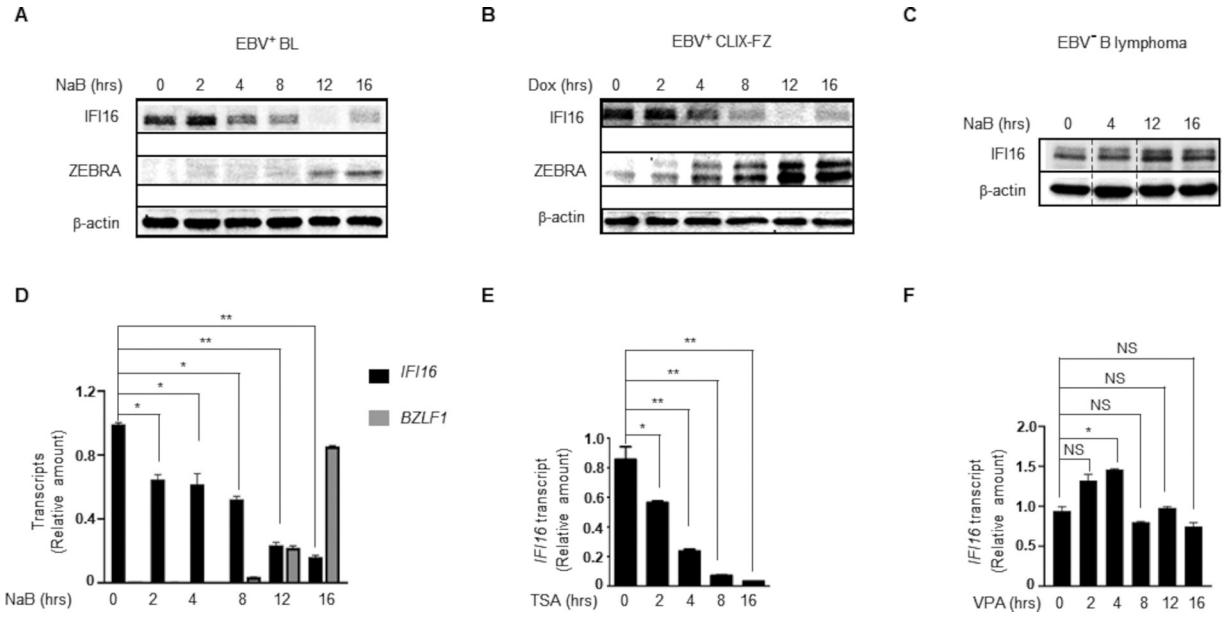

FIG 4 IFI16 message and protein abundance rapidly decrease with lytic cycle activation in EBV$^+$ BL cells. (A and B) HH514-16 (EBV$^+$ BL; A), CLIX-FZ (doxycycline-inducible EBV$^+$ BL; B), and EBV$^-$ B lymphoma (BJAB; C) cells were exposed to lytic triggers (NaB in A and C; doxycycline in B) for different durations followed by immunoblotting with indicated antibodies. (D to F) HH514-16 cells were induced with NaB (D), TSA (E), or VPA as mock induction control (F) for different durations followed by RT-qPCR analysis to determine the relative amounts of *IFI16* message after normalization to 18S rRNA using the $\Delta\Delta C_T$ method. Error bars, SEM of three technical replicates and two biological replicates; *, $P < 0.05$; **, $P < 0.01$; NS, not significant.

mammalian cells, constitutive heterochromatic regions are typically marked by H3K9me3 (35) and are predominantly found in extensively and permanently silenced regions, such as pericentromeric regions of chromosomes (36). However, the HCM that imposes H3K9me3 marks also silences foreign/invading DNA genomes, such as those of herpesviruses (23–25, 37). This machinery includes the core corepressor KAP1 that orchestrates the recruitment of several heterochromatin-inducing factors, including histone-lysine methyl transferases. The five known mammalian histone-lysine methyltransferases all bind KAP1 but act differentially on their H3 substrate (38–43). In the context of KSHV, IFI16 was found to recruit the methyltransferases SUV39H1 and GLP to trimethylate H3K9 on viral genes (16). However, whether IFI16 partners with the core HCM to recruit methyltransferases or functions independently of the core HCM during antiviral gene silencing is not known. In

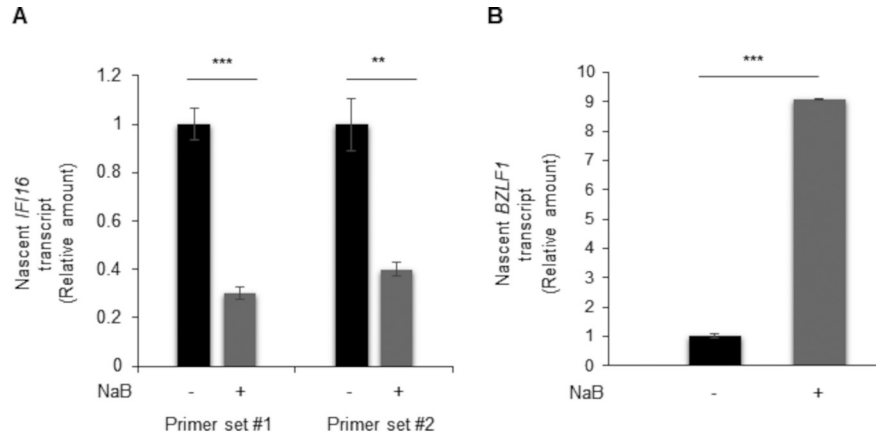

FIG 5 Reduced transcription contributes to a drop in abundance of *IFI16* messages after lytic cycle activation. HH514-16 BL cells were left untreated or induced with NaB for 10 h, before performing BrU-PCR. Nascent RNA was precipitated with an anti-BrdU antibody followed by RT-qPCR analysis with two primer sets (number 1 and number 2) to determine the relative amounts of newly synthesized *IFI16* message (A) and *BZLF1* message (B) after normalization to 18S rRNA. Error bars, SEM of three technical replicates and two biological replicates; **, $P < 0.01$; ***, $P < 0.001$; NS, not significant.

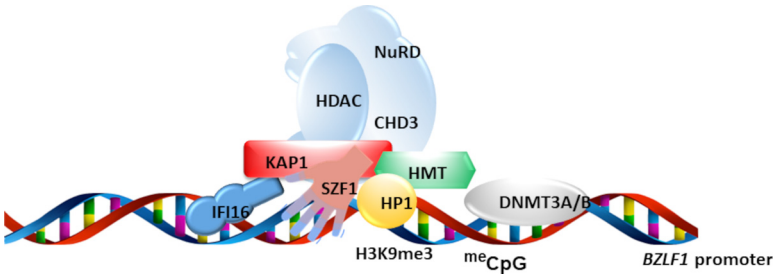

FIG 6 Model of IFI16's partnership with the constitutive heterochromatin machinery (HCM) that blocked EBV latent-to-lytic transition. N-terminal KRAB domain of the KRAB-ZFP SZF1 interacted with the corepressor KAP1 while C-terminal zinc fingers bind viral DNA. KAP1 recruited histone-lysine methyltransferases (HMT), the deacetylase complex NuRD-HDAC, and the heterochromatin amplification factor HP1 to silence target genes via H3K9me3 marks. Shown also is the proposed involvement of the DNA sensor IFI16 which directly contacts KAP1 but not SZF1.

the context of EBV, IFI16 also silences multiple viral lytic genes via H3K9 trimethylation (our results and those in reference (12)), the mechanism and IFI16's relationship with the core HCM remains unexplored. Our findings indicated a partnership between IFI16 and core members KAP1 and SZF1, the latter is known to recruit and specifically target KAP1 to SZF1-binding sites on EBV lytic genes. While our experiments found IFI16 complexed with (i) KAP1 on the *BZLF1* promoter and (ii) H3K9me3, as well as place IFI16 adjacent to KAP1 and KAP1 adjacent to SZF1 (27), IFI16 was bound to the HCM at some distance from SZF1 (Fig. 6). To our knowledge, this is the first time that IFI16 has been mechanistically and functionally linked to the core HCM.

Although IFI16 partners with the HCM, the need for two DNA binding proteins (SZF1 and IFI16) within/associated with the HCM is unclear. One possibility is that IFI16 recruits transcription factors so that lytic promoters are poised to begin gene expression upon disruption of the HCM. However, this is unlikely given the enhancement in lytic gene expression that we observed upon depletion of IFI16. Another possibility is that IFI16 recruits other repressors not typically recruited by the HCM to all or a subset of sites silenced by the HCM. A third possibility is that IFI16 excludes transcription factors. Exclusion of TBP and Oct 1 was observed in HSV-1 infected cells (3). A fourth possibility is that IFI16 redirects the HCM from consensus binding sites on the self/host genome to nonconsensus binding sites on viral genomes (24). Conversely, the HCM (SZF1) may provide IFI16 with selectivity in recognizing viral gene targets to discriminate from self/host DNA. Indeed, IFI16 is not known to bind specific DNA sequences, and binding to the HCM may facilitate IFI16's recognition of foreign over self-DNA. In that context, IFI16 may recognize self-DNA without the involvement of the core HCM.

In earlier studies, loss of IFI16 protein was observed late (>48 to 72 h) after lytic activation of both EBV and KSHV. While this loss was sensitive to inhibition of viral DNA replication in KSHV-infected cells (44), an immediate early or early lytic gene was thought to be responsible for IFI16 depletion in EBV-infected cells (12). Unlike our study, these studies did not detect an early loss of IFI16 likely because of a difference in the timing of investigation of the lytic phase. The early drop in the abundance of *IFI16* transcripts appears to be related to activation of the lytic cycle and not the presence of HDAC inhibition *per se*. That said also, the relevance of the short-chain fatty acid butyrate in this context cannot be dismissed because butyrate is produced by bacterial fermentation by gut microbes (45), resulting in ample exposure of infected B cells within the gut, the largest immune organ.

Our findings raised several questions, including whether IFI16 silenced the incoming EBV genome and was needed to establish EBV latency. Further, whether IFI16 partners with KAP1/the core HCM in distinguishing foreign from self is not known, and how IFI16 transcription was turned down in the prelytic phase remains to be explored.

MATERIALS AND METHODS

Cell lines and chemical treatment. EBV-positive Burkitt lymphoma (BL) cell lines (HH514-16, a kind gift from George Miller, Yale University, and Mutu I, a kind gift of Erik Flemington, Tulane University) and EBV-negative B lymphoma cell line (BJAB) were maintained in RPMI 1640 medium containing 10% fetal

bovine serum and 1% penicillin/streptomycin. The CLIX-FZ (Clone-HH514-16 transfected with pLIX_402-FZ) cell line (46), containing a stably integrated doxycycline-inducible tagged *BZLF1* gene, was maintained in RPMI 1640 medium containing 10% fetal bovine serum, 1% penicillin/streptomycin, and puromycin (P8833, Sigma-Aldrich). Cells were subcultured at 5×10^5 cells/mL, and 24 h later were induced with 3 mM (of 1 mM in Fig. 1B) sodium butyrate (NaB, 303410, Sigma-Aldrich), 10 mM valproic acid (VPA, P4543, Sigma-Aldrich), 5 μM trichostatin A (TSA, T8552, Sigma-Aldrich), or 5 ng/mL TGF-β1 (7754-BH-005, R&D systems).

Plasmids, siRNAs, and transfection. Cells were transfected with 200 pmol siRNA or 10 μg plasmids in transfection solution (MIR50117, Mirus) using an Amaxa Nucleofector II as described previously (47). siRNAs used in this study included those targeting *KAP1* (J-005046-07, Dharmacon) and *IFI16* (sc-35633, Santa Cruz Biotechnology; 107747, Thermo Fisher Scientific). Plasmids included IFI16 (a gift from Cheryl Arrowsmith, Addgene plasmid number 35064) and pcDNA5.1/FRT/TO empty vector (a kind gift from Torben Heick Jensen, Denmark).

Immunoblotting and antibodies. Immunoblotting was performed as previously described (24). Briefly, cells were lysed with RIPA buffer and electrophoresed in 10% SDS-polyacrylamide gels before performing immunostaining with indicated antibodies. Antibodies included: mouse anti-ZEBRA antibody (clone BZ1; a kind gift from Paul Farrell, Imperial College, London), mouse anti-β-actin antibody (AC-15, Sigma), rabbit anti-KAP1 antibody (A300-274A, Bethyl Laboratories), mouse anti-IFI16 antibody (sc-515790, Santa Cruz Biotechnology), rabbit anti-SZF1/ZNF589 antibody (PA5-68940, Thermo Fisher Scientific), mouse anti-H3K9me3 antibody (5327, Cell Signaling Technology), HRP-conjugated goat anti-mouse IgG(H+L) (626520, Thermo Fisher Scientific) and HRP-conjugated goat anti-rabbit IgG(H+L) (31460, Thermo Fisher Scientific).

Quantitative reverse transcriptase PCR (RT-qPCR). RT-qPCR was performed as previously described (48) and data were analyzed by normalizing to 18S rRNA using the $\Delta\Delta$CT method. PCR primers included the following: 5′GTAACCCGTTGAACCCCATT3′ (forward) and 5′CCATCCAATCGGTAGTAGCG3′ (reverse) for *18S* rRNA; 5′TTCCACAGCCTGCACCAGTG3′ (forward) and 5′GGCAGAAGCCACCTCACGGT3′ (reverse) for *BZLF1*; 5′AC CTGCCGTTGGATCTTAGTG3′ (forward) and 5′GGCGTTGTTGGAGTCCTGTG3′ (reverse) for *BMRF1*; 5′AACCAGA ATAATCTCCCCAATG3′ (forward) and 5′CGAGGCACCCCAAAAGTC3′ (reverse) for *BFRF3*; 5′ACAGACTCAGCCT CCCTC3′ (forward) and 5′ACTATCACTGGGCGTTTT3′ (reverse) for *IFI16*.

Proximity ligation assay (PLA) and immunofluorescence. PLA was performed as described previously (27, 46). Briefly, cells were fixed with Cytofix/Cytoperm solution (554722, BD Bioscience) for 15 min on ice followed by washing with 1× BD Perm/Wash buffer (554723, BD Bioscience) two times and subjected to incubation with indicated primary antibodies for 1 h. After washing two times, the cells were incubated with the PLUS and MINUS PLA probes (DUO92006 and DUO92002, Sigma-Aldrich) for 1 h and washed twice with buffer A (DUO82049, Sigma-Aldrich). Cells were then incubated with ligation reaction buffer (DUO94002, Sigma-Aldrich) for 30 min and washed twice with buffer A. Next, cells were incubated in amplification reaction for 100 min and washed twice with buffer B (DUO82049, Sigma-Aldrich). After a final wash with 1:100 buffer B, cells were subjected to second-round immunostaining with EBV seropositive reference serum for 1 h followed by secondary Allophycocyanin (APC) conjugated goat anti-human IgG incubation for 45 min. After two more washes, cells were mounted on slides with DAPI (P36935, Thermo Fisher Scientific). Images were acquired using a fluorescence microscope (OLYMPUS) and analyzed with Image Studio Lite software. Antibodies used for PLA included: goat anti-KAP1 antibody (A300-274A, Bethyl Laboratories), rabbit anti-IFI16 antibody (14970, Cell Signaling Technology), and rabbit anti-SZF1/ZNF589 antibody (PA5-68940, Thermo Fisher Scientific).

Bromouridine-RT-qPCR (Bru-qPCR) analysis. Bru-PCR was performed as described previously (34). Briefly, 10 million cells were left untreated or treated with 3 mM NaB. Cells were pulsed with 2 mM bromouridine (BrU, 850187, Sigma-Aldrich) at 37°C for 30 min before harvesting. RNA was isolated with RNeasy plus kit (74134, Qiagen) and then incubated with 0.1% bovine serum albumin (BSA) prewashed goat anti-mouse IgG magnetic Dynabeads (11033; Invitrogen) and 2 μg mouse anti-BrdU antibody (555627; BD Biosciences) together with 20 U RNasin (10777019; Invitrogen) for 1 h at room temperature. Beads were washed three times with 200 μL 0.1% BSA in DEPC-PBS containing 20 U RNasin. Samples were eluted by adding 40 μL nuclease-free water and incubated at 95°C for 10 min. The eluted nascent BrU-containing RNA was removed to a new Eppendorf tube and subjected to RT-qPCR analysis.

Primers used for Bru-qPCR included: primer set number 1, 5′TGGACCCAAAGGGAGTAAGG3′ (forward) and 5′ATGAGGTCTTGGGAGATGGG3′ (reverse); primer set number 2, 5′GGAGAAGTTCACCCCAAAGAAG3′ (forward) and 5′GCATTCACATCAGCCACAAG3′ (reverse) for amplifying adjacent intron-exon segments of *IFI16* transcripts and 5′GACCCATACCAGGTGCCTTTTG3′ (forward) and 5′GCACACAAGGCAAAGGAGCTTG3′ (reverse) for amplifying adjacent intron-exon segments of *BZLF1* transcripts.

Co-immunoprecipitation (Co-IP). Co-IP was performed as described previously (46, 47). Briefly, 1×10^7 cells were lysed with IP lysis buffer (87787, Thermo Scientific) for 15 min and spun down for 5 min at 4°C. Following this, 5% of precleared cell lysates were set aside as input. The rest was incubated with 3 μg of rabbit anti-KAP1 antibody or rabbit anti-IgG as control together with 30 μL of dynabeads Protein G (10003D, Thermo Scientific) at 4°C overnight. Beads were washed with lysis buffer three times before performing immunoblotting.

ChIP and ChIP-re-ChIP. ChIP was performed as described previously (27). Briefly, 4 million cells were left untreated or treated with NaB (with or without depletion of IFI16) for different durations before performing ChIP. For each ChIP, cells lysates were incubated with 3.5 μg of each rabbit anti-H3K9me3 antibody (13969S, Cell Signaling Technology; Fig. 2C and D bottom), mouse anti-H3K9me3 antibody (6F12, Cell Signaling Technology; Fig. 2D top and middle), control rabbit IgG (AB-105-C, R&D systems), or control mouse IgG (557273, BD Pharmingen) and 25 μL Protein G Magnetic Beads (9006, Cell Signaling Technology) at 4°C overnight. For each ChIP-re-ChIP, cell lysates were incubated with 15 μg Rabbit anti-KAP1 antibody (A300-274A, Bethyl Laboratories)

and 40 μL Protein G Magnetic Beads (9006, Cell Signaling Technology) at 4°C overnight. Eluted protein-chromatin complexes from the first round of ChIP were then subjected to a second round of ChIP with 5 μg of mouse anti-IFI16 antibody (sc-8023, Santa Cruz Biotechnology) and 40 μL Protein G magnetic beads. Precipitated chromatin was analyzed by qPCR with the following primers: 5′TTCAGCAAAGATAGCAAAGGT3′ (forward) and 5′ACTTCTGAAAACTGCCTCCT3′ (reverse) for analyzing the promoter of *BZLF1*; 5′CCTAGACTACAGGCCTC TGAGT3′ (forward) and 5′ACTCAGAGGCCTGTAGTCTAGG3′ (reverse) for analyzing the promoter of *BMRF1;* 5′TCCCGCCTCTTGGATGCCATCAT3′ (forward) and 5′CTGGCCTCTGTCCGCAAAGTTAAA3′ (reverse) for analyzing the promoter of *BFRF3*.

Quantitative PCR (qPCR) to quantitate EBV load. Cell-associated EBV DNA was prepared as previously described (46) and relative amounts of viral DNA were quantified using quantitative-PCR (qPCR) by amplifying the EBV BALF5 locus. To quantify relative amounts of released EBV particles, equal amounts of supernatants from cell cultures were subjected to DNase treatment followed by qPCR using primers targeting the EBV BALF5 locus as above. Relative EBV genome copy numbers were calculated using a standard curve qPCR with BACmid p2089 serving as a template. Briefly, released EBV particles from 18 μL of culture supernatant were treated with 1 μL DNase in 20 μL of 1$\times$ DNase buffer followed by inactivation of DNase. Of this, 2 μL was used for qPCR analysis using BALF5 primers as described previously (34).

Statistical analysis. *P* values were calculated by using an unpaired Student's *t* test to compare the means of two groups.

ACKNOWLEDGMENTS

T.R.F. was supported by a Ruth L. Kirschstein Predoctoral Individual National Research Service Award from the NIDCR, F31 DE031931. S.B.-M. and M.T.M. were supported by the Children's Miracle Network and the University of Florida. M.T.M had support from DHS S&T contract RSFR-19-00104 and S.B.-M. was supported by NIH grant R01 AI113134.

M.T.M. and S.B.-M. designed the study, H.X., X.L., B.A.R., I.A.A., T.R.F., K.Z., and L.E.D. acquired and analyzed the data, H.X., X.L., B.A.R., T.R.F., K.Z., L.E.D., M.T.M. and S.B.-M. interpreted the data, and H.X., B.A.R., and S.B.-M. wrote the manuscript.

We declare no conflict of interest.

REFERENCES

1. Gariano GR, Dell'Oste V, Bronzini M, Gatti D, Luganini A, De Andrea M, Gribaudo G, Gariglio M, Landolfo S. 2012. The intracellular DNA sensor IFI16 gene acts as restriction factor for human cytomegalovirus replication. PLoS Pathog 8:e1002498. https://doi.org/10.1371/journal.ppat.1002498.
2. Lo Cigno I, De Andrea M, Borgogna C, Albertini S, Landini MM, Peretti A, Johnson KE, Chandran B, Landolfo S, Gariglio M. 2015. The nuclear DNA sensor IFI16 acts as a restriction factor for human papillomavirus replication through epigenetic modifications of the viral promoters. J Virol 89:7506–7520. https://doi.org/10.1128/JVI.00013-15.
3. Johnson KE, Bottero V, Flaherty S, Dutta S, Singh VV, Chandran B. 2014. IFI16 restricts HSV-1 replication by accumulating on the hsv-1 genome, repressing HSV-1 gene expression, and directly or indirectly modulating histone modifications. PLoS Pathog 10:e1004503. https://doi.org/10.1371/journal.ppat.1004503.
4. Abe T, Marutani Y, Shoji I. 2019. Cytosolic DNA-sensing immune response and viral infection. Microbiol Immunol 63:51–64. https://doi.org/10.1111/1348-0421.12669.
5. Diner BA, Lum KK, Cristea IM. 2015. The emerging role of nuclear viral DNA sensors. J Biol Chem 290:26412–26421. https://doi.org/10.1074/jbc.R115.652289.
6. Ansari MA, Singh VV, Dutta S, Veettil MV, Dutta D, Chikoti L, Lu J, Everly D, Chandran B. 2013. Constitutive interferon-inducible protein 16-inflammasome activation during Epstein-Barr virus latency I, II, and III in B and epithelial cells. J Virol 87:8606–8623. https://doi.org/10.1128/JVI.00805-13.
7. Kerur N, Veettil MV, Sharma-Walia N, Bottero V, Sadagopan S, Otageri P, Chandran B. 2011. IFI16 acts as a nuclear pathogen sensor to induce the inflammasome in response to Kaposi Sarcoma-associated herpesvirus infection. Cell Host Microbe 9:363–375. https://doi.org/10.1016/j.chom.2011.04.008.
8. Li T, Chen J, Cristea IM. 2013. Human cytomegalovirus tegument protein pUL83 inhibits IFI16-mediated DNA sensing for immune evasion. Cell Host Microbe 14:591–599. https://doi.org/10.1016/j.chom.2013.10.007.
9. Li T, Diner BA, Chen J, Cristea IM. 2012. Acetylation modulates cellular distribution and DNA sensing ability of interferon-inducible protein IFI16. Proc Natl Acad Sci U S A 109:10558–10563. https://doi.org/10.1073/pnas.1203447109.
10. Orzalli MH, Conwell SE, Berrios C, DeCaprio JA, Knipe DM. 2013. Nuclear interferon-inducible protein 16 promotes silencing of herpesviral and transfected DNA. Proc Natl Acad Sci U S A 110:E4492–E4501. https://doi.org/10.1073/pnas.1316194110.
11. Orzalli MH, DeLuca NA, Knipe DM. 2012. Nuclear IFI16 induction of IRF-3 signaling during herpesviral infection and degradation of IFI16 by the viral ICP0 protein. Proc Natl Acad Sci U S A 109:E3008–E3017. https://doi.org/10.1073/pnas.1211302109.
12. Pisano G, Roy A, Ahmed Ansari M, Kumar B, Chikoti L, Chandran B. 2017. Interferon-gamma-inducible protein 16 (IFI16) is required for the maintenance of Epstein-Barr virus latency. Virol J 14:221. https://doi.org/10.1186/s12985-017-0891-5.
13. Unterholzner L, Keating SE, Baran M, Horan KA, Jensen SB, Sharma S, Sirois CM, Jin T, Latz E, Xiao TS, Fitzgerald KA, Paludan SR, Bowie AG. 2010. IFI16 is an innate immune sensor for intracellular DNA. Nat Immunol 11:997–1004. https://doi.org/10.1038/ni.1932.
14. Merkl PE, Knipe DM. 2019. Role for a filamentous nuclear assembly of IFI16, DNA, and host factors in restriction of herpesviral infection. mBio 10:e02621-18. https://doi.org/10.1128/mBio.02621-18.
15. Lum KK, Howard TR, Pan C, Cristea IM. 2019. Charge-mediated pyrin oligomerization nucleates antiviral IFI16 sensing of herpesvirus DNA. mBio 10:e01428-19. https://doi.org/10.1128/mBio.01428-19.
16. Roy A, Ghosh A, Kumar B, Chandran B. 2019. IFI16, a nuclear innate immune DNA sensor, mediates epigenetic silencing of herpesvirus genomes by its association with H3K9 methyltransferases SUV39H1 and GLP. Elife 8:e49500. https://doi.org/10.7554/eLife.49500.
17. Thorley-Lawson DA, Gross A. 2004. Persistence of the Epstein-Barr virus and the origins of associated lymphomas. N Engl J Med 350:1328–1337. https://doi.org/10.1056/NEJMra032015.
18. Farrell PJ. 2019. Epstein-Barr virus and cancer. Annu Rev Pathol 14:29–53. https://doi.org/10.1146/annurev-pathmechdis-012418-013023.
19. Young LS, Rickinson AB. 2004. Epstein-Barr virus: 40 years on. Nat Rev Cancer 4:757–768. https://doi.org/10.1038/nrc1452.
20. Bjornevik K, Cortese M, Healy BC, Kuhle J, Mina MJ, Leng Y, Elledge SJ, Niebuhr DW, Scher AI, Munger KL, Ascherio A. 2022. Longitudinal analysis reveals high prevalence of Epstein-Barr virus associated with multiple sclerosis. Science 375:296–301. https://doi.org/10.1126/science.abj8222.
21. Hacohen Y, Ciccarelli O. 2022. New evidence for EBV infection as a cause of multiple sclerosis. Neurology 98:605–606. https://doi.org/10.1212/WNL.0000000000200243.
22. Robinson WH, Steinman L. 2022. Epstein-Barr virus and multiple sclerosis. Science 375:264–265. https://doi.org/10.1126/science.abm7930.

23. Bhaduri-McIntosh S, McIntosh MT. 2021. Inflammasome, the constitutive heterochromatin machinery, and replication of an oncogenic herpesvirus. Viruses 13:846–811. https://doi.org/10.3390/v13050846.
24. Burton EM, Akinyemi IA, Frey TR, Xu H, Li X, Su LJ, Zhi J, McIntosh MT, Bhaduri-McIntosh S. 2021. A heterochromatin inducing protein differentially recognizes self versus foreign genomes. PLoS Pathog 17:e1009447. https://doi.org/10.1371/journal.ppat.1009447.
25. Chang PC, Fitzgerald LD, Van Geelen A, Izumiya Y, Ellison TJ, Wang DH, Ann DK, Luciw PA, Kung HJ. 2009. Kruppel-associated box domain-associated protein-1 as a latency regulator for Kaposi's sarcoma-associated herpesvirus and its modulation by the viral protein kinase. Cancer Res 69:5681–5689. https://doi.org/10.1158/0008-5472.CAN-08-4570.
26. King CA, Li X, Barbachano-Guerrero A, Bhaduri-McIntosh S. 2015. STAT3 regulates lytic activation of Kaposi's sarcoma-associated herpesvirus. J Virol 89:11347–11355. https://doi.org/10.1128/JVI.02008-15.
27. Li X, Burton EM, Koganti S, Zhi J, Doyle F, Tenenbaum SA, Horn B, Bhaduri-McIntosh S. 2018. KRAB-ZFP repressors enforce quiescence of oncogenic human herpesviruses. J Virol 92:e00298-18. https://doi.org/10.1128/JVI.00298-18.
28. Bhaduri-McIntosh S, Miller G. 2006. Cells lytically infected with Epstein-Barr virus are detected and separable by immunoglobulins from EBV-seropositive individuals. J Virol Methods 137:103–114. https://doi.org/10.1016/j.jviromet.2006.06.006.
29. Daigle D, Megyola C, El-Guindy A, Gradoville L, Tuck D, Miller G, Bhaduri-McIntosh S. 2010. Upregulation of STAT3 marks Burkitt lymphoma cells refractory to Epstein-Barr virus lytic cycle induction by HDAC inhibitors. J Virol 84:993–1004. https://doi.org/10.1128/JVI.01745-09.
30. Hill ER, Koganti S, Zhi J, Megyola C, Freeman AF, Palendira U, Tangye SG, Farrell PJ, Bhaduri-McIntosh S. 2013. Signal transducer and activator of transcription 3 limits Epstein-Barr virus lytic activation in B lymphocytes. J Virol 87:11438–11446. https://doi.org/10.1128/JVI.01762-13.
31. Fredriksson S, Gullberg M, Jarvius J, Olsson C, Pietras K, Gustafsdottir SM, Ostman A, Landegren U. 2002. Protein detection using proximity-dependent DNA ligation assays. Nat Biotechnol 20:473–477. https://doi.org/10.1038/nbt0502-473.
32. Countryman JK, Gradoville L, Miller G. 2008. Histone hyperacetylation occurs on promoters of lytic cycle regulatory genes in Epstein-Barr virus-infected cell lines which are refractory to disruption of latency by histone deacetylase inhibitors. J Virol 82:4706–4719. https://doi.org/10.1128/JVI.00116-08.
33. Burton EM, Goldbach-Mansky R, Bhaduri-McIntosh S. 2020. A promiscuous inflammasome sparks replication of a common tumor virus. Proc Natl Acad Sci U S A 117:1722–1730. https://doi.org/10.1073/pnas.1919133117.
34. Frey TR, Brathwaite J, Li X, Burgula S, Akinyemi IA, Agarwal S, Burton EM, Ljungman M, McIntosh MT, Bhaduri-McIntosh S. 2020. Nascent transcriptomics reveal cellular prolytic factors upregulated upstream of the latent-to-lytic switch protein of Epstein-Barr virus. J Virol 94:e01966-19. https://doi.org/10.1128/JVI.01966-19.
35. Martens JH, O'Sullivan RJ, Braunschweig U, Opravil S, Radolf M, Steinlein P, Jenuwein T. 2005. The profile of repeat-associated histone lysine methylation states in the mouse epigenome. EMBO J 24:800–812. https://doi.org/10.1038/sj.emboj.7600545.
36. Klement K, Goodarzi AA. 2014. DNA double strand break responses and chromatin alterations within the aging cell. Exp Cell Res 329:42–52. https://doi.org/10.1016/j.yexcr.2014.09.003.
37. Rauwel B, Jang SM, Cassano M, Kapopoulou A, Barde I, Trono D. 2015. Release of human cytomegalovirus from latency by a KAP1/TRIM28 phosphorylation switch. Elife 4:e06068. https://doi.org/10.7554/eLife.06068.
38. Schultz DC, Ayyanathan K, Negorev D, Maul GG, Rauscher FJ 3rd, 2002. SETDB1: a novel KAP-1-associated histone H3, lysine 9-specific methyltransferase that contributes to HP1-mediated silencing of euchromatic genes by KRAB zinc-finger proteins. Genes Dev 16:919–932. https://doi.org/10.1101/gad.973302.
39. Loyola A, Tagami H, Bonaldi T, Roche D, Quivy JP, Imhof A, Nakatani Y, Dent SY, Almouzni G. 2009. The HP1alpha-CAF1-SetDB1-containing complex provides H3K9me1 for Suv39-mediated K9me3 in pericentric heterochromatin. EMBO Rep 10:769–775. https://doi.org/10.1038/embor.2009.90.
40. Rea S, Eisenhaber F, O'Carroll D, Strahl BD, Sun ZW, Schmid M, Opravil S, Mechtler K, Ponting CP, Allis CD, Jenuwein T. 2000. Regulation of chromatin structure by site-specific histone H3 methyltransferases. Nature 406:593–599. https://doi.org/10.1038/35020506.
41. Rivera C, Saavedra F, Alvarez F, Diaz-Celis C, Ugalde V, Li J, Forne I, Gurard-Levin ZA, Almouzni G, Imhof A, Loyola A. 2015. Methylation of histone H3 lysine 9 occurs during translation. Nucleic Acids Res 43:9097–9106. https://doi.org/10.1093/nar/gkv929.
42. Tachibana M, Sugimoto K, Fukushima T, Shinkai Y. 2001. Set domain-containing protein, G9a, is a novel lysine-preferring mammalian histone methyltransferase with hyperactivity and specific selectivity to lysines 9 and 27 of histone H3. J Biol Chem 276:25309–25317. https://doi.org/10.1074/jbc.M101914200.
43. Tachibana M, Ueda J, Fukuda M, Takeda N, Ohta T, Iwanari H, Sakihama T, Kodama T, Hamakubo T, Shinkai Y. 2005. Histone methyltransferases G9a and GLP form heteromeric complexes and are both crucial for methylation of euchromatin at H3-K9. Genes Dev 19:815–826. https://doi.org/10.1101/gad.1284005.
44. Roy A, Dutta D, Iqbal J, Pisano G, Gjyshi O, Ansari MA, Kumar B, Chandran B. 2016. Nuclear innate immune DNA sensor IFI16 is degraded during lytic reactivation of Kaposi's sarcoma-associated herpesvirus (KSHV): role of IFI16 in maintenance of KSHV latency. J Virol 90:8822–8841. https://doi.org/10.1128/JVI.01003-16.
45. Donohoe DR, Garge N, Zhang X, Sun W, O'Connell TM, Bunger MK, Bultman SJ. 2011. The microbiome and butyrate regulate energy metabolism and autophagy in the mammalian colon. Cell Metab 13:517–526. https://doi.org/10.1016/j.cmet.2011.02.018.
46. Li X, Burton EM, Bhaduri-McIntosh S. 2017. Chloroquine triggers Epstein-Barr virus replication through phosphorylation of KAP1/TRIM28 in Burkitt lymphoma cells. PLoS Pathog 13:e1006249. https://doi.org/10.1371/journal.ppat.1006249.
47. Xu H, Perez RD, Frey TR, Burton EM, Mannemuddhu S, Haley JD, McIntosh MT, Bhaduri-McIntosh S. 2019. Novel replisome-associated proteins at cellular replication forks in EBV-transformed B lymphocytes. PLoS Pathog 15:e1008228. https://doi.org/10.1371/journal.ppat.1008228.
48. Mannemuddhu SS, Xu H, Bleck CKE, Tjandra N, Carter C, Bhaduri-McIntosh S. 2021. Prazoles targeting Tsg101 inhibit release of Epstein-Barr virus following reactivation from latency. J Virol 95:e0246620. https://doi.org/10.1128/JVI.02466-20.